Two-Way Power Divider With Wide Tunable Power Ratio Range for Weighted-Polarization MIMO Antenna in BAN Radios at 2.45 GHz

Taiyang Xie, *Graduate Student Member, IEEE*, Ruiya Shi, *Graduate Student Member, IEEE*, Shuai Wang, Xiaolong Wang, *Member, IEEE*, Kazuhiro Honda, *Member, IEEE*, Kun Li, *Member, IEEE*, and Geyu Lu

***Abstract*—This study presented an implementation of weighted-polarization multiple-input–multiple-output (MIMO) antenna for wireless body area networks at 2.45 GHz. The weight function determined by considering the variation in the cross-polarization power ratio *(XPR)* and the antenna tilt angle was realized by a two-way power divider (PD), where tunable power ratio range of proposed PD could not only cross the boundary of equal power ratio ($k^2 = 1$), but also maintain a wide tunable range at the same time. The patch array antenna fed by the proposed PD consists of microstrip lines, capacitors, resistors, and varactor diodes can overcome the polarization mismatch in dynamic off-body channel due to the variation in radio-propagation environment and human movement by adjusting the bias voltages. The experiment of 2×2 MIMO channel capacity was conducted using a three-dimensional spatial fading emulator. The measured and simulated results are in good agreement. Under the considered condition of arm-swinging angle and the *XPR*, the tunable power ratio range of proposed PD can be realized from -1.25 dB to 20 dB; therefore, it is suitable for radio-frequency control antenna to obtaining high data transmission in future wearable MIMO applications.**

***Index Terms*—Body area network, channel capacity, cross-polarization power ratio *(XPR)*, multiple-input–multiple-output (MIMO), off-body channel, over-the-air testing, power divider.**

I. Introduction

THE increasing demand of medical-healthcare devices has accelerated the development of wireless body area networks (BANs) [1], [2]. BAN systems are generally comprised of body-worn and implantable sensor devices that operate in the immediate vicinity or inside of the human body using radio-frequency (RF) technologies. Based on different operational bandwidths, wireless communications systems in BAN radios can be classified into narrowband [3] and wideband [4], respectively. In narrowband system, the frequency operated at industrial, scientific and medical band, such as 400 MHz, 900 MHz, and 2.45 GHz bands. They are usually employed for lower bit rate transmission in medical wireless system [5]−[7], such as electroencephalogram (EEG), electrocardiogram (ECG), and endoscopic images. On the other hand, the use of millimeter wave frequencies in wearable applications has also been paid great attention [8], the bio-medical information can be detected and delivered from these wearable devices to external terminals and cellular base stations for health management in general life environment.

Based on this off-body communication scenario with the main purpose of portable medical devices, there are two main technical subjects in BAN radios. The first issue is the dynamic channel variation caused by human motion [9]. Especially for watch-type or pedometer-type terminals that mounted on the limbs or joints of human body, the polarization properties of wearable antennas will be readily changed due to human walking motion [10], [11]. The other important issue is the radio-wave propagation environment in medical-healthcare use scenarios [12]. Unlike cellular system, medical devices such as vital sensors are generally used in hospital building and sickroom, where the distance between local base station and wearable terminals is relatively small. Thus, cross-polarization power ratio (*XPR*) may vary significantly where line-of-sight (LOS) and non-LOS (NLOS) channels are alternately generated. Moreover, multipath radio components due to the reflections and diffractions from surrounding furniture and walls may occur, which eventually results in fast fading phenomenon when human body moves in a distance [13], [14]. Therefore, the development of high-speed communication wearable antennas with the function of overcoming polarization mismatch and multipath fading is imperative.

An 8×8 weighted-polarization wearable multiple-input–multiple-output (MIMO) antenna for BAN dynamic channel at 2 GHz has been reported in [15]. By using three-orthogonally arranged dipoles [16] or three-axis antenna with disk-loaded patch configuration [17], the effectiveness of derived weigh function for power ratio control of cross-polarization components has been confirmed. However, the weight circuit in the preliminary experiment was realized by adjusting external phase shifters and attenuators. The structure of weight circuit part is heavy and inconvenient, and it can only achieve a limited combination of weight functions.

Therefore, power divider (PD) with tunable power ratio is a potential solution for weight circuit realization. Several unequal

Manuscript received February 23, 2022; accepted April 10, 2022. Date of publication April 13, 2022; date of current version July 7, 2022. This work was supported in part by Project of the Education Department of Jilin Province under Grant JJKH20211093KJ; in part by Interdisciplinary Integration and Innovation Project of JLU under Grant JLUXKJC2020204; and in part by the Project of Science and Technology Development Program of Changchun City under Grant 21ZY23. *(Corresponding author: Xiaolong Wang.)*

Taiyang Xie, Ruiya Shi, Shuai Wang, Xiaolong Wang, and Geyu Lu are with the State Key Laboratory of Integrated Optoelectronics, College of Electronic Science and Engineering, International Center of Future Science, Jilin University, Changchun 130012, China (e-mail: brucewang@jlu.edu.cn; smalld729@hotmail.com).

Kazuhiro Honda is with the Graduate School of Engineering, Toyama University, Toyama 930-8555, Japan.

Kun Li is with the Faculty of Engineering and Design, Kagawa University, Takamatsu 761-0396, Japan.

Digital Object Identifier 10.1109/LAWP.2022.3167099

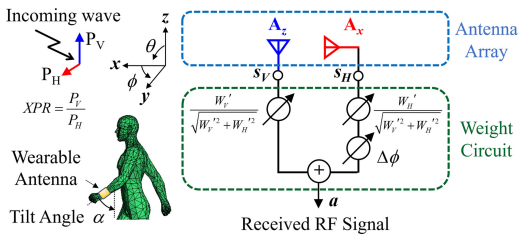

Fig. 1. Concept of weighted-polarization RF control antenna for off-body wireless communication.

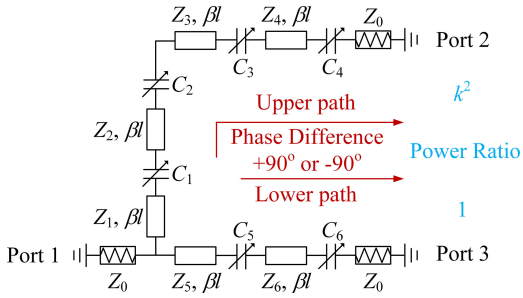

Fig. 2. Topology of proposed PD.

PDs [18]−[21] have been introduced with tunable power ratio k^2. However, $k^2 = 1$ is a clear boundary, where the range of k^2 must be larger than 1 or smaller than 1. So far as we know, no unequal PD has been reported to cross this boundary. Although quasi-lumped quadrature coupler with two varactor diodes can be used for changing power ratio, its phase difference is naturally shifted from 0° to −55°. To sum up, no tunable PD has been developed for weight circuit application to achieve the following performances: first, cross the power ratio boundary of $k^2 = 1$; and second, controllable 90° phase difference.

In this letter, two-way PD with wide tunable power ratio range is newly presented to achieve weight function combinations for BAN off-body radios at 2.45 GHz. The theoretical power ratio range of proposed PD could not only cross the boundary of $k^2 = 1$, but also reach to -10 dB $< k^2 <$ 20 dB, therefore, such kind of tunable PD has not been reported in any former works. Based on a statistical analysis of arm-swinging behavior in a human walking motion [11], the range of $-20° < \alpha < 50°$ is utilized in this study, where α is antenna tilt angle. By adjusting the bias voltages of varactors, the tunable power ratio range can be realized from −1.25 to 20 dB. Therefore, the weighted-polarization antenna can overcome the polarization mismatch in dynamic BAN channel due to the variation in *XPR* and antenna tilt angle. The over-the-air (OTA) testing of 2 × 2 MIMO channel capacity confirmed the validity of proposed PD for obtaining high and stable data transmission in future wearable MIMO applications.

II. Principle of Weighted-Polarization and Its Realization

A. Weighted-Polarization RF Control

Fig. 1 shows the original concept of deriving weigh function for dynamic off-body channels [16]. Two orthogonally arranged antenna elements (A_z and A_x) are controlled by weight function for realization of different power ratios, which takes the *XPR* and antenna tilt angle α as key parameters. The signal received at the output port is expressed as follows:

$$a = \frac{W_V{}'}{\sqrt{W_V{}'^2 + W_H{}'^2}} s_V + \frac{W_H{}'}{\sqrt{W_V{}'^2 + W_H{}'^2}} s_H e^{j\Delta\phi} \quad (1)$$

where $W_V{}' = W_V|\cos\alpha| + W_H|\sin\alpha|$, $W_H{}' = W_V|\sin\alpha| + W_H|\cos\alpha|$, s_V and s_H denote the received signals of A_z and A_x, respectively.

A phase term of $\Delta\phi = \pi/2$ is added to eliminate the enhancement and cancellation of vertical and horizontal polarization components when the antenna is tilted by arm movement. The weight functions (W_V, W_H) at each antenna branch can be calculated by the allotment of the signal according to the *XPR*, as given by

$$W_V = \sqrt{XPR/(1+XPR)} \text{ and } W_H = \sqrt{1/(1+XPR)}. \quad (2)$$

In order to obtain the optimum received signal at any antenna inclination angle, the dominant incoming wave polarization can be determined by using (1) and (2), where, the derivation method of (1) has been described in [16] in details.

B. Realization of Weight Circuit by Proposed PD

Fig. 2 shows the topology of proposed PD which consists of six similar segments. Because power ratio between ports 2 and 3 is k^2:1, we have $k = W_V{}'/W_H{}'$. For each segment, there is one varactor with capacitance C_N and single transmission line with characteristic impedance Z_N and electrical length βl, where N = 1, 2, 3, 4, 5, 6.

From single segment, we have

$$\begin{bmatrix} A_N & B_N \\ C_N & D_N \end{bmatrix} = \begin{bmatrix} \cos(\beta l) & jZ_N \sin(\beta l) \\ j\sin(\beta l)/Z_N & \cos(\beta l) \end{bmatrix} \begin{bmatrix} 1 & 1/jH_N \\ 0 & 1 \end{bmatrix} \quad (3)$$

where $H_N = 1/\omega_0 C_N$.

The upper and lower paths of proposed PD can be summarized as follows:

$$\begin{bmatrix} A_{Up} & B_{Up} \\ C_{Up} & D_{Up} \end{bmatrix} = \begin{bmatrix} A_1 & B_1 \\ C_1 & D_1 \end{bmatrix} \begin{bmatrix} A_2 & B_2 \\ C_2 & D_2 \end{bmatrix} \begin{bmatrix} A_3 & B_3 \\ C_3 & D_3 \end{bmatrix} \begin{bmatrix} A_4 & B_4 \\ C_4 & D_4 \end{bmatrix} \quad (4a)$$

$$\begin{bmatrix} A_{Low} & B_{Low} \\ C_{Low} & D_{Low} \end{bmatrix} = \begin{bmatrix} A_5 & B_5 \\ C_5 & D_5 \end{bmatrix} \begin{bmatrix} A_6 & B_6 \\ C_6 & D_6 \end{bmatrix} \quad (4b)$$

Then, Z matrix of proposed PD can be calculated by (5) shown at the bottom of the next page.

Because *S*-parameter can be derived from

$$S = (Z+E)^{-1}(Z-E) \quad (6)$$

where E is 3 × 3 identity matrix.

In order to realize the desired weight function, the following equations must be maintained.

$$S_{11} = 0, \quad k^2|S_{12}|^2 = |S_{13}|^2 \text{ and } \angle S_{12} - \angle S_{13} = \pm 90^\circ. \quad (7)$$

After complicated arithmetical operation, the relationship between six characteristic impedances and six capacitances of varactors can be finally determined. In other words, when C_4 and C_5 are given, other four capacitances can be calculated by the following equations:

$$C_1 = 1/H_1\omega_0,\ C_2 = 1/H_2\omega_0,\ C_3 = 1/H_3\omega_0 \text{ and } C_6 = 1/H_6\omega_0 \quad (8)$$

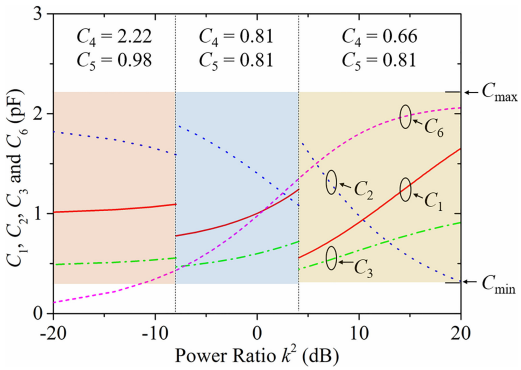

Fig. 3. Tunable power ratio range of proposed PD.

where

$$H_6 = \frac{\sqrt{k^2 Z_6^2 - k^2 Z_5^2 + Z_6^2}}{kZ_5},\ H_2 = \frac{kZ_2Z_3Z_5\left(H_4H_6+1\right)}{Z_1Z_4Z_6} \quad (9a)$$

$$H_3 = \frac{Z_4\left(Z_1Z_3Z_6 + kZ_2Z_4Z_5H_6\right)}{kZ_2Z_5\left(H_4H_6+1\right)},\ H_4 = 1/\omega_0 C_4,\ H_5 = 1/\omega_0 C_5 \quad (9b)$$

$$H_1 = \frac{Z_2^2}{H_2} - \frac{H_5 Z_1^2}{Z_5^2} + \frac{H_6 Z_1^2 k^2}{(1+k^2)} + \frac{(H_6 - H_4)\, Z_1Z_2Z_3Z_5k}{H_2Z_4Z_6\,(1+k^2)}. \quad (9c)$$

In order to achieve a wide tunable power ratio range, a set of values of six characteristic impedances (Z_1, Z_2, Z_3, Z_4, Z_5, and Z_6) are finally selected, which are 90 Ω, 50 Ω, 50 Ω, 80 Ω, 85 Ω, and 100 Ω respectively. Power ratio range vs. capacitances of varactors is shown in Fig. 3. When the capacitances range of the six varactors (SMV2019-040LF) is from $C_{\min}$ (0.30 pF) to $C_{\max}$ (2.22 pF), obviously, the power ratio k^2 can be achieved from −10 to 20 dB theoretically. Comparing with the former works [18]−[22], the tunable power ratio range of proposed work could not only cross the boundary of $k^2 = 1$, but also maintain a wide tunable range at the same time. Considering the variation range of α and *XPR*, the power ratio range of weight circuit should be limited from −1.25 to 20 dB.

Based on the discussion above, a two-way tunable PD is newly designed for weight-polarization antenna application. Fig. 4(a) shows photograph of 2 × 2 weight-polarization MIMO antenna, which is fabricated on a Rogers RT/5880 substrate. Each antenna is comprised of the proposed two-way tunable PD and a rectangular patch element. The layout of tunable PD with a patch antenna is shown in Fig. 4(b). All the physical sizes and substrate information are labeled in details. In addition, Fig. 4(b) also shows the three-dimensional (3-D) view of weight-polarization antenna created by HFSS software. The position and circuit model with all variable diode (C_1 - C_6) in the HFSS simulation are marked.

The antenna impedance was measured by a Keysight Technologies 8753ES vector network analyzer. For the reflection coefficient (S_{11}, S_{22}) of the proposed antenna, both the measured and simulated results are lower than −28.6 dB at 2.45 GHz when $\alpha = 0$ and $XPR = 20$ dB. In the tunable power ratio range for

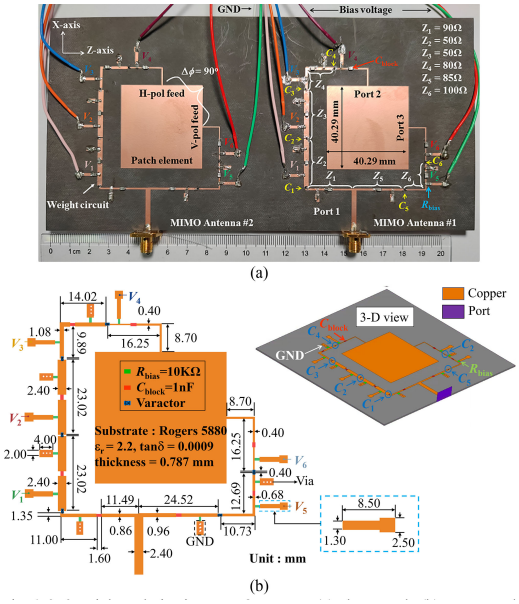

Fig. 4. 2 × 2 weight-polarization MIMO antenna. (a) Photograph. (b) Layout and its HFSS 3-D view of a single element of proposed MIMO antenna with details of PD part.

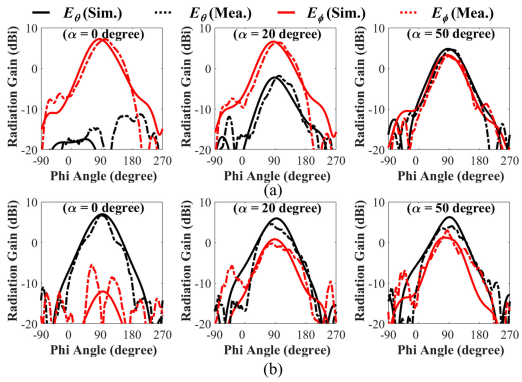

Fig. 5. Radiation patterns at *xy*-plane in different antenna tilt angle α considering a radio wave environment of $XPR = 20$ dB. (a) Horizontally polarized patch antenna. (b) Weight-polarization patch antenna.

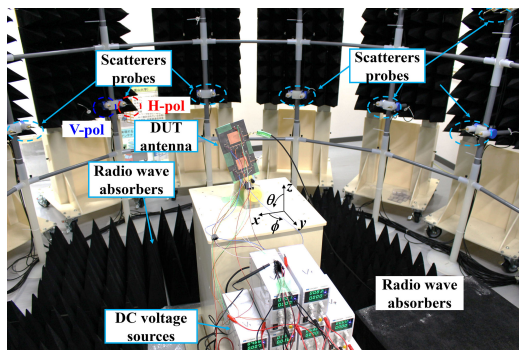

Fig. 6. 3-D spatial fading emulator for a 2 × 2 MIMO channel capacity experiment when the *XPR* is set to 20 dB.

$$Z = \frac{1}{(A_{\text{Low}}C_{Up} + A_{Up}C_{\text{Low}})} \begin{bmatrix} A_{Up}A_{Low} & A_{Low} & A_{Up} \\ A_{Low} & (A_{Low}D_{Up} + B_{Up}C_{Low}) & 1 \\ A_{Up} & 1 & (A_{Up}D_{Low} + B_{Low}C_{Up}) \end{bmatrix}. \quad (5)$$

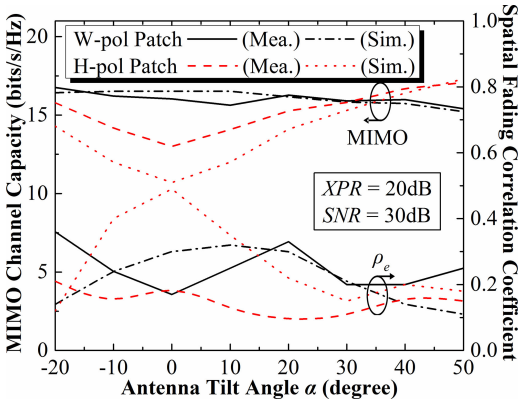

Fig. 7. Measurement and simulation results of 2×2 MIMO channel capacity and spatial fading correlation coefficient ρ_e as a function of antenna tilt angles α when $XPR = 20$ dB.

realizing the desired weight functions, the reflection coefficients of proposed antenna cannot exceed -15.7 dB. Through the experimental verification of the power divider part, the tunable power ratio range can be realized from 17.6 dB ($\alpha = 0°$) to -11.9 dB ($\alpha = 80°$). The abovementioned facts indicate that the combined structure of the two-way PD and the patch antenna is well designed.

III. Antenna Evaluation

To validate the proposed design of PD, the performance of fabricated weighted-polarization MIMO antenna in Fig. 4(a) was evaluated. For comparison with the proposed antenna, a 2-element MIMO antenna comprised of similar dimension of patch element fed by horizontal polarization wave was used.

A. Radiation Pattern

Fig. 5 shows the measured and simulated results radiation patterns for one of the MIMO antenna elements at *xy*-plane. The measured radiation performance was obtained in a microwave anechoic chamber at Tsinghua University. Fig. 5(a) and (b) indicates the results of weighted-polarization patch and horizontally polarized patch antenna, respectively. The cases for the antenna tilt angle α at 0°, 20°, and 50° were investigated. The *XPR* of 20 dB was considered for validating the proposed antenna, indicating a radio-propagation environment dominated by vertically polarized incident waves. In Fig. 5(a), when the horizontally polarized patch antennas were used, a strong E_ϕ component is observed. This is obviously undesirable in a θ-polarized radio-propagation environment, i.e., $XPR = 20$ dB. On the other hand, when the proposed weighted-polarization antenna is used, as shown in Fig. 5(b), a large E_θ component in each antenna tilt angle is realized and maintained by the adjusting appropriate weight functions using the proposed two-way PD. The measured radiation patterns are in good agreement with the simulated results by HFSS software, indicating that the performance of proposed antenna is kept in good condition according to the *XPR* and antenna tilt angle α.

B. 2×2 MIMO Channel Capacity

Fig. 6 illustrates a MIMO-OTA apparatus for channel capacity measurement at Toyama University. The device of test (DUT) antenna was located at the center of a 3-D spatial fading emulator with a cylindrical configuration. The 14×3 scatterers probes composed of cross-polarized spertopf dipole antennas were used to emulate the desired *XPR* and angular power distribution of the incident wave of uniform in azimuth and Gaussian in elevation. In the experiment, both the average incident angle and angular spread in elevation were set to 20°. The *XPR* and signal-to-noise ratio *(SNR)* was set to 20 dB and 30 dB, respectively. The system calibration of power loss due to the incident wave and *XPR* control unit was conducted [23].

Fig. 7 shows the measured and simulated results of 2×2 MIMO channel capacity and spatial correlation coefficient [24] as a function of antenna tilt angles α. The simulated results were calculated by the Monte Carlo simulation based on a 3-D channel model [25].

As can be seen in Fig. 7, when the proposed antenna with appropriate weight functions is used, a high and stable channel capacity is achieved regardless of the antenna tilt angle α. On the other hand, when the horizontally polarized patch antenna is used, significant degradations can be observed due to the absence of the receiving ability for the θ-polarized components. As the angle increases up to 50°, due to the reversal of antenna polarization, the original horizontally polarized antenna will become more capable of receiving θ-component of incident wave power, resulting in a higher channel capacity compared with the proposed antenna. The above results demonstrate that the weight functions controlled by the two-way tunable PD work well in different conditions of α. On the one hand, from $-20°$ to 40°, the maximum difference of MIMO channel capacity compared with horizontally polarized patch is 2.9 bits/s/Hz. Based on Shannon's Theorem, it implies that the proposed 2×2 MIMO antenna can achieve up to 4.4 dB of total RF power improvement compared with that of the horizontally polarized patch antenna, which can eventually overcome the combined polarization mismatch caused by variation of human dynamic motion in this angular region and the *XPR*. In addition, when $\alpha = 50°$, a small deviation of measured channel capacity between the proposed antenna and horizontally polarized antenna is shown. The reason can be attributed to the fact that the measured result of maximum E_θ component at $\alpha = 50°$ is slightly degraded, as shown in Fig. 5(b). On the other hand, in the range of antenna tilt angle considered in this study, both the measured and simulated spatial correlation coefficient ρ_e between two antenna elements show the entire low levels of less than 0.4, which permits the MIMO channel capacity of the proposed weighted-polarization antenna to increase in a multipath Rayleigh fading environment.

IV. Conclusion

This study presented a two-way PD with a wide tunable power ratio range for realizing weighted-polarization control of wearable MIMO antenna in dynamic BAN radios at 2.45 GHz. The effectiveness of proposed structure of the PD was confirm to overcome the polarization mismatch in dynamic off-body channel due to the variation in *XPR* and human dynamic motion by the MIMO channel capacity experiment in an OTA evaluation. Future studies will focus on the realization of large-scale MIMO antennas with optimized structure of PD in wearable medical device, including practical experiments using realistic human phantom.

References

[1] P. S. Hall and Y. Hao, *Antennas and Propagation for Body-Centric Wireless Communications*. London, U.K.: Artech House, 2006.

[2] R. Chavez-Santiago *et al.*, "Propagation models for IEEE 802.15.6 standardization of implant communication in body area networks," *IEEE Commun. Mag.*, vol. 51, no. 8, pp. 80–87, Aug. 2013.
[3] X. Y. Zhang, H. Wong, T. Mo, and Y. F. Cao, "Dual-band dual-mode button antenna for on-body and off-body communications," *IEEE Trans. Biomed. Circuits Syst.*, vol. 11, no. 4, pp. 933–941, Aug. 2017.
[4] Q. Wang, T. Tayamachi, I. Kimura, and J. Wang, "An on-body channel model for UWB body area communications for various postures," *IEEE Trans. Antennas Propag.*, vol. 57, no. 4, pp. 991–998, Apr. 2009.
[5] M. Gallo, P. S. Hall, Y. I. Nechayev, and M. Bozzetti, "Use of animation software in simulation of on-body communications channels at 2.45 GHz," *IEEE Antennas Wireless Propag. Lett.*, vol. 7, pp. 321–324, 2008.
[6] G. A. Conway and W. G. Scanlon, "Antennas for over-body-surface communication at 2.45 GHz," *IEEE Trans. Antennas Propag.*, vol. 57, no. 4, pp. 844–855, Apr. 2009.
[7] A. Ruaro, J. Thaysen, and K. B. Jakobsen, "Wearable shell antenna for 2.4 GHz hearing instruments," *IEEE Trans. Antennas Propag.*, vol. 64, no. 6, pp. 2127–2135, Jun. 2016.
[8] R. Aminzadeh, A. Thielens, M. Zhadobov, L. Martens, and W. Joseph, "WBAN channel modeling for 900 MHz and 60 GHz communications," *IEEE Trans. Antennas Propag.*, vol. 69, no. 7, pp. 4083–4092, Jul. 2021.
[9] N. Yamamoto, N. Shirakata, D. Kobayashi, K. Honda, and K. Ogawa, "BAN radio link characterization using an arm-swinging dynamic phantom replicating human walking motion," *IEEE Trans. Antennas Propag.*, vol. 61, no. 8, pp. 4315–4326, Aug. 2013.
[10] K. Honda, K. Li, and K. Ogawa, "Shadowing-fading BER characterization of a BAN diversity antenna based on statistical measurements of the human walking motion," *IEICE Trans. Commun.*, vol. 96, no. 10, pp. 2530–2541, Oct. 2013.
[11] K. Li, K. Honda, and K. Ogawa, "Analysis of the body proximity cross-polarization power ratio in a human walking motion," in *Proc. Asia-Pacific Microw. Conf., Session TU4F*, Nanjing, China, Dec. 2015, vol. 2, pp. 1–3.
[12] S. L. Cotton, "A statistical model for shadowed body-centric communications channels: Theory and validation," *IEEE Trans. Antennas Propag.*, vol. 62, no. 3, pp. 1416–1424, Mar. 2014.
[13] K. Li, K. Honda, and K. Ogawa, "Rice channel realization for BAN over-the-air testing using a fading emulator with an arm-swinging dynamic phantom," *IEICE Trans. Commun.*, vol. 98, no. 4, pp. 543–553, Apr. 2015.
[14] K. Li, K. Honda, and K. Ogawa, "Dual-discrete processing for bit-error-rate OTA testing in shadowing-fading BAN channel," *IEEE Antennas Wireless Propag. Lett.*, vol. 16, pp. 1200–1204, 2017.
[15] K. Honda, K. Li, and K. Ogawa, "An 8 × 8 MIMO 3-axis weighted polarization active antenna for wearable radio applications," in *Proc. 31th URSI Gen. Assem. Sci. Symp.*, Beijing, China, Aug. 2014, vol. 1, no. 17, pp. 1–4.
[16] K. Honda, K. Li, and K. Ogawa, "Weighted-polarization wearable MIMO antenna with three orthogonally arranged dipoles based on RF signal processing," *IEICE Trans. Commun.*, vol. 99, no. 1, pp. 58–68, Jan. 2016.
[17] H. Sato, K. Omote, K. Li, K. Honda, Y. Koyanagi, and K. Ogawa, "The 3-axis polarization antenna using disk-loaded monopole stacked with patch antenna in PCB," in *Proc. Asia-Pacific Microw. Conf.*, Nanjing, China, Dec. 2015, vol. 1, pp. 1–3.
[18] H. Fan, X. Liang, J. Geng, R. Jin, and X. Zhou, "Reconfigurable unequal power divider with a high dividing ratio," *IEEE Microw. Wireless Compon. Lett.*, vol. 25, no. 8, pp. 514–516, Aug. 2015.
[19] L. Guo, H. Zhu, and A. M. Abbosh, "Wideband tunable in-phase power divider using three-line coupled structure," *IEEE Microw. Wireless Compon. Lett.*, vol. 26, no. 6, pp. 404–406, Jun. 2016.
[20] E. Al Abbas, A. M. Abbosh, and K. Bialkowski, "Tunable in-phase power divider for 5G cellular networks," *IEEE Microw. Wireless Compon. Lett.*, vol. 27, no. 6, pp. 551–553, Jun. 2017.
[21] X. T. Ye, W. T. Li, C. Cui, and X. W. Shi, "A continuously tunable unequal power divider with wide tuning range of dividing ratio," *IEEE Microw. Wireless Compon. Lett.*, vol. 28, no. 7, pp. 567–569, Jul. 2018.
[22] Y.-S. Liu and J.-S. Row, "Back-to-back microstrip antenna fed with tunable power divider," *IEEE Trans. Antennas Propag.*, vol. 63, no. 5, pp. 2348–2353, May 2015.
[23] K. Honda and K. Li, "Three-dimensional MIMO-OTA calibration to achieve the Gaussian angular power spectra in elevation," *IEICE Commun. Exp.*, vol. 5, no. 10, pp. 394–400, Oct. 2016.
[24] K. Ogawa, A. Yamamoto, and J.-I. Takada, "Multipath performance of handset adaptive array antennas in the vicinity of a human operator," *IEEE Trans. Antennas Propag.*, vol. 53, no. 8, pp. 2422–2436, Aug. 2005.
[25] K. Li, K. Honda, and K. Ogawa, "Three-dimensional over-the-air assessment for vertically arranged MIMO array antennas," *IEICE Trans. Commun.*, vol. E99-B, no. 1, pp. 167–176, Jan. 2016.